



PROFESSOR RUTH ESTELA ROSENSTEIN (Orcid ID : 0000-0002-8804-4395)

DR DAMIAN DORFMAN (Orcid ID : 0000-0002-7967-9866)

Article type : Original Manuscript

MELATONIN PROTECTS THE RETINA FROM EXPERIMENTAL NON-EXUDATIVE AGE-RELATED MACULAR DEGENERATION IN MICE

Hernán H. Diéguez¹, María F. González Fleitas¹, Marcos L. Aranda¹, Juan S. Calanni¹, María I. Keller Sarmiento¹, Mónica S. Chianelli¹, Agustina Alaimo², Pablo H. Sande¹, Horacio E. Romeo³, Ruth E. Rosenstein¹, Damián Dorfman¹

Running title: Macular degeneration and melatonin

1. Laboratory of Retinal Neurochemistry and Experimental Ophthalmology, Department of Human Biochemistry, School of Medicine/CEFyBO, University of Buenos Aires/CONICET, Buenos Aires, Argentina. 2. Interdisciplinary Laboratory of Cellular Dynamics and Nanotools, Department of Biological Chemistry, School of Exact and Natural Sciences/IQUIBICEN, University of Buenos Aires/CONICET, Buenos Aires. 3. School of Engineering and Agrarian Sciences, Pontifical Catholic University of Argentina, BIOMED/UCA/CONICET, Buenos Aires, Argentina.

Corresponding author: Dr. Damián Dorfman
Departamento de Bioquímica Humana
Facultad de Medicina/CEFyBO,
UBA/CONICET,

This article has been accepted for publication and undergone full peer review but has not been through the copyediting, typesetting, pagination and proofreading process, which may lead to differences between this version and the [Version of Record](#). Please cite this article as [doi: 10.1111/JPL.12643](https://doi.org/10.1111/JPL.12643)

This article is protected by copyright. All rights reserved

Paraguay 2155, 5° P, (1121)
Buenos Aires, ARGENTINA
Phone n°: 54-11-5285-3252
FAX n°: 54-11-4508-3672 (ext. 31)
e-mail: ddorfman@fmed.uba.ar

ABSTRACT

Non-exudative age-related macular degeneration (NE-AMD) represents the leading cause of blindness in the elderly. Currently, there are no available treatments for NE-AMD. We have developed a NE-AMD model induced by superior cervical ganglionectomy (SCGx) in C57BL/6J mice, which reproduces the disease hallmarks. Several lines of evidence strongly support the involvement of oxidative stress in NE-AMD-induced retinal pigment epithelium (RPE) and outer retina damage. Melatonin is a proven and safe antioxidant. Our aim was analyzing the effect of melatonin in the RPE/outer retina damage within experimental NE-AMD. The treatment with melatonin starting 48 h after SCGx, which had no effect on the ubiquitous choriocapillaris widening, protected visual functions, and avoided Bruch's membrane thickening, RPE melanin content, melanosome number loss, retinoid isomerohydrolase (RPE65)-immunoreactivity decrease, and RPE and photoreceptor ultrastructural damage induced within experimental NE-AMD exclusively located at the central temporal (but not nasal) region. Melatonin also prevented the increase in outer retina/RPE oxidative stress markers, and a decrease in mitochondrial mass at 6 weeks post-SCGx. Moreover, when the treatment with melatonin started at 4 weeks post-SCGx, it restored visual functions and reversed the decrease in RPE melanin content and RPE65-immunoreactivity. These findings suggest that melatonin could become a promising safe therapeutic strategy for NE-AMD.

Key words: non-exudative age-related macular degeneration; melatonin; superior cervical ganglion; retinal pigment epithelium; oxidative stress.

INTRODUCTION

Non-exudative age-related macular degeneration (NE-AMD) is the leading cause of irreversible blindness in the elderly worldwide, affecting ~ 9% of the global population, and thought to almost duplicate by 2040 [1, 2]. Within NE-AMD, the atrophy of the retinal pigment epithelium (RPE) and photoreceptors (PR) occur, exclusively localized at the central retinal region (i.e., the macular area). Clinically, NE-AMD appears as a progressive defect in central vision, leading to legal blindness. Many factors are related to the development and progression of NE-AMD; female gender, age, diet, cigarette smoking, and Caucasian race among others, have been implicated in NE-AMD development and progression [1, 3, 4]. Moreover, factors such as choroidal blood flow impairment, the accumulation of lipofuscin at the RPE, oxidative stress, and inflammation have been related to the etiopathogenesis of NE-AMD [5-7]. Several studies indicate that oxidative stress damaging the RPE is an early phenomenon in NE-AMD [1, 7-12]. So far, based on the AREDS I and II clinical trials, the only available therapeutic approach is the supplementation with high doses of antioxidants, vitamins, and zinc (reviewed in [13]). However, both the complex formulation and the high antioxidants and vitamins doses make their long-term use unsafe and, on top of that, their use does not achieve conclusive results [14].

We have recently developed a new model of NE-AMD induced by superior cervical ganglionectomy (SCGx) in C57Bl/6J mice, which reproduces the central features of human NE-AMD. SCGx induces a decline in PR function, and ubiquitous alterations in the choroid and choriocapillaris, whereas the increase in Bruch's membrane (BrM) thickness, the decrease in the content of RPE melanin and retinoid isomerohydrolase (RPE65)-immunoreactivity, the occurrence of drusen-like deposits, and the atrophy of the RPE and PR are localized exclusively at the temporal region of the optic nerve head [15]. Moreover, SCGx induces an increase in several markers of oxidative stress, and a decrease both in the central temporal (without any nasal alterations) RPE mitochondria mass, and endogenous antioxidant system enzymes [16]. Melatonin is a molecule with proven antioxidant and anti-inflammatory activities, which reduces oxidative stress and inflammatory cell damage often underlying neurodegenerative disorders (reviewed in [17-19]). Evidence strongly supports that melatonin and its metabolites act both as direct and indirect antioxidants by free radicals scavengers, antioxidant enzymes stimulators, and other antioxidants activities enhancers [20-24]. Melatonin may also act as a shield in other ocular afflictions such as cataract, photo-keratitis, prematurity retinopathy, and injury due to ischemia/reperfusion [25-27], as well as refractory central serous chorioretinopathy in humans [28]. We have previously exposed the benefits of the treatment with melatonin against glaucoma [29], uveitis [30-32], type-2 diabetes mellitus-induced retinal

damage [33], and optic neuritis [34]. In this context, the purpose of our work was analysing melatonin therapeutic effect on the RPE and outer retina damage in SCGx-induced NE-AMD.

MATERIALS AND METHODS

Animals

For all experiments adult male C57BL/6J mice (weighting an average of 27 ± 3 g and ageing an average of 2.5 ± 0.5 months) were kept in a standard animal room, and fed with food and water *ad libitum* under controlled conditions of temperature, light, and humidity, in a 12-hour light/12-hour dark cycle. A total number of 138 animals were used, as follows: 30 for electroretinogram (ERG), melanin content and immunofluorescence studies, 10 for electron microscopy, 16 for MitoTracker and MitoSOX studies, 32 for Western blot, 10 behaviour visual tests, and 40 for analyzing a delayed treatment with melatonin. This study was approved by the ethics committee of the School of Medicine, University of Buenos Aires (Institutional Committee for the Care and Use of Laboratory Animals, (CICUAL), and animal suffering was minimized with all efforts. Intramuscular injection of 100 mg/kg ketamine hydrochloride and 2 mg/kg xylazine hydrochloride was used for every experimental procedure anesthesia.

Superior cervical ganglionectomy

The left superior cervical ganglion (SCG) was aseptically removed through a ventral midline incision in the neck, as previously described [15]. For all experiments but the behaviour visual tests, we conducted a simulated procedure (i.e., non-removing the right SCG), thus considering the right eye as control (from then on named sham). No differences between eyes from sham-treated animals and naïve animals were found along our studies [15, 16].

Melatonin treatment

Using a bronzed cylinder of 2.5 mm diameter and 1 mm length, we achieved a pellet of melatonin (20 mg in 3 % w/v vegetable oil), which was subcutaneously implanted 48 h or 4 weeks post-SCGx, and replaced every 10 days, based on previous reports [29, 31, 34]. Another group of animals was sham-operated (without the pellet implant (further named control)).

ERG recording

Standard scotopic electroretinograms were assessed using a HMsERG model 2000 (Ocuscience LLC, Kansas City, MO, USA) equipped with a Ganzfield dome. Light stimulus was done with a fitted white-light-emitting-diode at an eye distance of 2 cm, as previously described [15,16]. Briefly, 15 (2 ms each)

full-field 10 cd/sm² flashes at a frequency of 0.25 Hz were averaged for each animal, and the mean of 10 animals was taken as representative for each group.

Behavior visual tests

A looming and visual cliff tests were used to evaluate visual functions. The looming and visual cliff tests were performed as described by Lim et al. [35]. The freezing latency and response to stimulus were analyzed. The virtual visual cliff test was performed as described by Gu et al. [36]. Animals were subjected to unilateral SCGx or sham procedure, while the contralateral eye remained intact. After 48 h or 4 weeks (delayed treatment), some animals received melatonin, whereas others were operated without the pellet implant (control). A number of 10 mice/group were used for each test, which in the case of the looming test was performed only once for each mouse to avoid habituation.

Electron microscopy

Using an ultramicrotome Ultracut E (Reichert-Jung, Vienna, Austria), we obtained ultrathin retinal sections (50 nm) from the central nasal and temporal region (at 800 μ m from the optic nerve head (ONH)), as previously described [15, 16]. For orientation (nasal/temporal axis), nictitating membrane was left attached to the eye, and a clean cut was made through the horizontal meridian including in each half both the ONH and the nictitating membrane. After mounting on 300 Mesh grids, sections were stained with uranyl acetate (2% in 70% ethanol) and Reynolds lead citrate, and observed and photographed using a Zeiss 109T transmission electron microscope (Carl Zeiss Microscopy, Peabody, MA, USA) equipped with a digital camera (ES1000W; Gatan, Pleasanton, CA, USA). RPE ultrastructural damage was evaluated using a 1-4 scale: 1 = no detectable damage; 2 = increase in basal infoldings thickness; 3 = melanosome number decrease; 4 = vacuolization. PR ultrastructural damage was quantified using a 1-4 scale: 1 = no detectable damage; 2 = loss of double membrane; 3 = discs disorganization; 4 = electron dense material presence.

RPE melanin content quantification

After deparaffination and dehydration, sections were mounted in slides covered with slips using Canada balsam as previously described [15, 16]. Light microscopic images (\times 1000) from the total RPE section were obtained at equidistant eccentricities from the ONH (taken as zero) to the nasal or temporal periphery each 200 μ m long. The content of RPE melanin was quantified at 800 μ m nasally and temporally of the ONH using ImageJ software version 1.42q (NIH, Bethesda, MD, USA). The average from four separate sections per eye, and the mean of five eyes was recorded as the representative value for each group.

Immunofluorescence studies

Animals were intracardially perfused with saline, followed by 4% paraformaldehyde in PBS and paraffin sections were obtained and mounted in superfrost microscope slides (Erie Scientific Company, Portsmouth, New Hampshire, USA), as previously described [15, 16]. Sections were preincubated with 5% normal horse serum for 1 h and then were incubated overnight at 4°C with a mouse polyclonal anti-RPE65 antibody (1:500; EMD Millipore, Darmstadt, Germany, MAB5428), a mouse monoclonal anti-4-hydroxy-2-nonenal (4HNE) (1:250, R&D Systems, Minneapolis, MN, USA), or a mouse monoclonal anti-carboxymethyl-lysine (CML) (1:250, R&D Systems, Minneapolis, MN, USA). The following secondary antibodies were added, and incubated for 2 h at room temperature: a goat anti-mouse IgM secondary antibody conjugated to Alexa Fluor 568 (1:500; Invitrogen, Molecular Probes, Carlsbad, CA, USA, A11031). Nuclei were stained with Hoechst (1 µg/ml Sigma Chemical Co., St Louis, MO, USA), and observed under an epifluorescence microscope (BX50; Olympus, Tokyo, Japan) with a video camera attached to a computer running image analysis software (Image-Pro Plus, Media Cybernetics Inc., Bethesda, USA). All retinal images shown were oriented with the vitreous up. The RPE65 (+) area was quantified using ImageJ software version 1.42q (NIH, Bethesda, MD, USA). For each eye, we analysed 4 separate sections from the RPE at the central nasal and temporal region and the mean from 5 different eyes/group was considered the representative value.

Ex vivo flat-mounted RPE mitochondrial labelling and superoxide detection

We obtained flat-mounts of the RPE incubated them either with MitoTracker-Red CMXRos (500 nM) (Molecular Probes, Eugene, OR, USA) for 15 minutes in mammalian ringer (MR) buffer or with MitoSOX-Red (5 µM) (Molecular Probes, Eugene, OR, USA) for 30 minutes in MR buffer at 37°C under red dim light, as we described [15, 16]. Samples were observed under an epifluorescent microscope (BX-50, Olympus, Tokyo, Japan). The (+) area of both markers was quantified using ImageJ software version 1.42q (NIH, Bethesda, MD, USA). For each group, we analysed 4 images from the RPE at the central nasal and temporal region and the mean from 4 different eyes/group was considered the representative value.

Tissue harvesting for SDS-PAGE and Western blotting

After enucleation, the retina was delicately detached from the RPE followed by the separately homogenization of each tissue (retina and RPE/choroid) as we have previously described [16]. Using bovine serum albumin as the standard, the protein content was determined following the method of Lowry

et al. [37]. Proteins (50 µg/sample) were separated by SDS-PAGE 12%. Proteins were then transferred to polyvinylidenedifluoride membranes (60 min at 100 V in a Bio-Rad Trans-Blot SD system (Bio-Rad Laboratories, Hercules, CA, USA)). Membranes were then incubated (overnight at 4°C) with the following antibodies: a mouse monoclonal anti-cytochrome c (1:1000, Santa Cruz Biotechnology, Dallas TX, USA), a rabbit polyclonal anti-traslocase of the outer membrane (TOM20, 1:500, Santa Cruz Biotechnology, Dallas, TX, USA), a rabbit polyclonal anti-voltage-dependent selective-anion channel (VDAC) (1:300, Santa Cruz Biotechnology, Dallas, TX, USA), and a mouse anti-β-actin (1:1000, Santa Cruz Biotechnology, Dallas, TX, USA). The following secondary antibodies were used: a donkey anti-mouse (1:2000, Jackson Laboratory, Bar Harbor, ME, USA) and a donkey anti rabbit (1:2000, Jackson Laboratory, Bar Harbor, ME, USA). Enhanced chemiluminescence Western blotting detection reagents were used to visualize immunoblots (Amersham Biosciences, Buenos Aires, Argentina). ImageQuant software was used to quantify densitometric signals adjusted by the density of β-actin. For each group, the mean of 4 homogenates were averaged and taken as the representative value.

Statistical analysis

Statistical analysis of results was made by a two-way analysis of variance (ANOVA) followed by a Tukey's test, as stated, and met the necessary assumptions. The assumption of equal variances was tested by the F-test. In every statistical analysis, $P < 0.05$ was considered statistically significant.

RESULTS

Visual functions were assessed by ERG recording, and three visual tests (i.e., looming, virtual visual cliff, and visual cliff) in sham- and SCGx-animals, and in the absence or presence of melatonin starting at 48 h post-SCGx. SCGx induced a significant decrease in scotopic ERG a-wave amplitude and in the looming, virtual visual cliff, and visual cliff test responses at 10 weeks post-surgery. The treatment with melatonin, which had no effect *per se*, completely prevented the visual dysfunctions (Figure 1). Figure 2 shows representative ultraphotomicrographs of the central nasal and temporal choriocapillaris at 10 weeks post-surgery. The treatment with melatonin had no effect on the ubiquitous increase in choriocapillaris lumen height increase at either region, both in sham-treated or SCGx-subjected eyes (Figure 2). However, melatonin prevented the SCGx-induced alterations in BrM ultrastructure, showing dense fibrillary collagen deposits within the elastic layer, an increase in RPE and endothelial cell basal membrane thickness, and BrM thickening only at the temporal region (Figure 3). Photomicrographs and ultraphotomicrographs representative of each group at the central nasal and temporal RPE are shown in Figure 4. Melatonin prevented the decrease in RPE melanin and melanosome content in the temporal region induced by SCGx

at 10 weeks post-surgery. In addition, SCGx-induced a significant decrease in RPE65-immunoreactivity circumscribed to the temporal RPE, which was completely prevented by melatonin (Figure 5). The ultrastructural analysis showed RPE vacuolization and a clear disorganization of the PR membranous discs, blebs and complete disc loss, replaced by amorphous electron-dense material localized at the temporal region at 10 weeks post-SCGx, which were not observed in SCGx-submitted eyes from melatonin-treated animals, as shown in Figure 6. Oxidative stress markers were analysed at 6 weeks post-surgery. The treatment with melatonin completely prevented the increase in 4HNE- and CML-immunoreactivity at the temporal RPE and PR outer segments and RPE, respectively, induced by SCGx (Figure 7). In addition, melatonin significantly prevented the SCGx-induced increase in the temporal RPE mitochondria superoxide content (assessed with MitoSOX-Red probe), and the decrease in MitoTracker-Red-labelled mitochondria (an index of mitochondrial mass) (Figure 8). Moreover, melatonin prevented the SCGx-induced decrease in the levels of intrinsic mitochondrial proteins (i.e., cytochrome c, VDAC and TOM20) exclusively at the temporal RPE, as shown in Figure 9. The results shown above, demonstrate that the treatment with melatonin starting at 48 h post-SCGx prevented the damage induced by experimental NE-AMD. When melatonin treatment started at 4 weeks post-SCGx, it completely reversed the visual dysfunctions (ERG, and visual tests) induced by SCGx at 10 weeks post-surgery, as shown in Figure 10, as well as the decrease in temporal RPE melanin content and RPE65-immunoreactivity (Figure 11).

DISCUSSION

For the first time, the foregoing results demonstrate that melatonin provided functional and structural protection to the RPE and outer retina in experimental NE-AMD. In particular, melatonin preserved the ERG a-wave amplitude, the visual test performances, and the BrM, the RPE and the PR ultrastructure. In accordance with previous studies both in rats and mice, SCGx induces ubiquitous choroid alterations [11, 15, 16, 38]. However, all but the choriocapillaris alterations found within NE-AMD induced by SGCx were exclusively located at the central temporal area of the outer retina/RPE, an area that according to Volland and co-workers [39], shows human-like cone/rod ratio, the highest concentration of cones, and the specialization of the RPE and Bruch's membrane (BrM) in C57BL/6J mice, making it comparable to the human macula. Moreover, biochemical and structural differences between the nasal and temporal region could account for the localized damage induced by SCGx [15, 16]. Experimental NE-AMD induced by SCGx can be divided in two phases: an early phase (up to 6 weeks post-SCGx), characterized by PR dysfunction (ERG a-wave), BrM thickening, decreased RPE melanin content, and RPE65-immunoreactivity, subtle ultrastructural RPE and PR alterations, increase in oxidation markers (4HNE,

CML, MitoSOX), and mitochondria mass decrease, followed by a late phase (at 10 weeks post-SCGx), at which severe RPE ultrastructural damage and PR loss become evident [15]. These alterations cannot be attributed to a denervation-related decrease in pineal gland-synthesized melatonin, since SCGx induces ubiquitous alterations in the choroid and choriocapillaris, while exclusively circumscribed changes in the PR, BrM, and RPE localized at the central temporal region, and because no differences between the contralateral eye and naïve eyes are observed [15].

In the present report, we chose to analyse the effect of melatonin on NE-AMD outcomes at 10 weeks post-SCGx so as to maximize the damage in the RPE/outer retina function and histology, thus allowing us to discard the possibility of melatonin inducing a transient protection. Melatonin was administered as subcutaneous pellets, which secured reaching continuous dosing and reduced the animal manipulation associated with a daily administration. Moreover, we have already shown in previous reports the success of this dosing and administration way to achieve retinal and optic nerve protection against several experimental visual diseases [29, 33, 34].

Electroretinography is a method to objectively evaluate the retinal function. The treatment with melatonin prevented the decrease in the scotopic ERG a-wave amplitude induced by SCGx, supporting that melatonin protected PR function. Since ERG only provides reliable information on the electrical retinal response to a flash of light, vision being a much more complex function, we assessed the effect of SCGx and melatonin on three behavioural tests, thus evaluating visual functions from a broader perspective. The looming response is a reflex relying exclusively on visual cues [40] that evaluates the integrity of the retino-colicular pathway, while both the visual and the virtual visual cliff tests evaluate binocular depth perception as a result of the functional integrity of the retino-geniculo-cortical pathway [36, 41]. SCGx induced a decrease in the performance of these behavioural tests, while the treatment with melatonin preserved visual functions.

Although melatonin was unable to modify the choriocapillaris lumen height increase induced by SCGx, it significantly prevented alterations in BrM thickness and ultrastructure in SCGx-eyes. Bruch's membrane, formerly considered a *passive* structure lying between the RPE and the choroid, actually constitutes altogether with the choriocapillaris and the RPE a single functional cluster [42], strategically located, and allowing hydraulic homeostasis, metabolic waste disposal and nutrient transport between systemic circulation, and avascular outer retina. It has been demonstrated that BrM thickening leads to RPE and PR damage [43, 44]. Regardless it is not yet clear whether BrM alterations lead to RPE damage or *vice versa*, the treatment with melatonin protected the BrM either as a primary effect or as a consequence of RPE protection.

Melanin, a pigment concentrated in the choroid and the RPE, has a central role in removing radiation excess, and reactive oxygen species (ROS) derived from RPE metabolism [45]. Thus, a decrease in the RPE melanin content might lead to a deficit in quenching both high-energy photons and ROS, and in turn, to an increase in oxidative stress. RPE65, an isomerohydrolase specifically located in the RPE, produces 11-cis-retinol from all-trans-retinyl esters, is a key player in the visual cycle. Melatonin prevented the decrease in RPE melanin content and RPE65-immunoreactivity at the central temporal region induced by SCGx.

The mechanisms involved in the therapeutic effect of melatonin remain to be established. NE-AMD is a complex disease involving several pathological mechanisms; still, oxidative stress, particularly acting at the central temporal RPE, seems to play a pivotal role in its onset and progression. Excess of mitochondria-derived ROS due to mitochondria malfunction has been considered an early event in human and experimental NE-AMD [1, 16, 46, 47]. Moreover, gene polymorphisms related to oxidized base repair proteins [48], and increased mitochondrial DNA damage [49] have been found in AMD patients. Furthermore, decreased mitochondrial mass and mitochondria ultrastructure alterations in AMD specimens [46], and retinal degeneration in a RPE *sod2* mutant mouse [11] have been described. According to our results, melatonin prevented the increase in lipid peroxidation, mitochondria superoxide levels, and the decrease in mitochondria mass induced by SCGx, supporting that melatonin protected RPE/PR function and structure through its antioxidant activity. Consistently with our results, it has been reported that melatonin can exert protection against RPE cells oxidative damage and cell death induced by ischemia [50-53]. In addition, melatonin has shown to rescue mitochondria functionality by reducing oxidative stress and increasing mitochondria biogenesis in diabetic myocardial ischemia/reperfusion damage [54]. There are reports showing melatonin exerts its protective effects against oxidative stress through MT1 and/or MT2 receptors [55, 56]; however, receptor-independent antioxidant effects of melatonin have also been described [57, 58]. At present, we cannot ascertain whether the protective effect of melatonin against NE-AMD involves receptor-dependent or receptor-independent mechanisms, an issue that will be analysed in the near future.

The fact that the treatment with melatonin started 48 h after SCGx could limit the potential clinical translation of these results. Therefore, in order to analyse whether melatonin could not only prevent, but also slow or reverse NE-AMD progression, in another set of animals we started melatonin treatment at 4 weeks post-SCGx, a time-point at which functional and structural alterations are already evident [15]. The delayed treatment with melatonin reversed functional damage (ERG and behaviour visual tests), and achieved a complete protection of RPE melanin content and RPE65-immunoreactivity, thus being capable

of actively suppressing ongoing pathological mechanisms in experimental NE-AMD. In line with our results, in a single non-randomized clinical trial, it has been shown that the treatment with melatonin decreased the progression of AMD [59], reverses macular oedema, and improves visual acuity within human refractory central serous chorioretinopathy [28], a complex disease associated to an RPE dysfunction.

Overall, our results demonstrate that melatonin is capable of significantly preserve visual functions and retinal structure in experimental NE-AMD. Therefore, despite the well-known differences between the mouse and human retina, the treatment with melatonin, a very safe compound which lacks proven adverse effects even at high doses in humans [60], could become a promising therapy to prevent, slow down or even reverse RPE/retinal damages caused by human NE-AMD.

Author Contributions

Hernán H. Dieguez: design/concept, data acquisition, interpretation/data analysis; María F. González Fleitas: data acquisition; Marcos L. Aranda: data acquisition; Juan S. Calanni: data acquisition; María I. Keller Sarmiento: data acquisition; Mónica S. Chianelli: data acquisition; Pablo H. Sande: data acquisition; Horacio E. Romeo: data acquisition; Ruth E. Rosenstein: design/concept, interpretation/data analysis, manuscript drafting; Damián Dorfman: design/concept, interpretation/data analysis, manuscript drafting, and article final approval.

Acknowledgments

The following funding fonts were used in this work: Agencia Nacional de Promoción Científica y Tecnológica [PICT 1563, PICT 2731]; Universidad de Buenos Aires [20020100100678]; Consejo Nacional de Investigaciones Científicas y Técnicas [PIP 0707], Argentina. Neither the design nor the performance of this work was influenced by the funding sources. No interest conflicts are reported by any of the authors of this work.

REFERENCES

[1] Datta, S., Cano, M., Ebrahimi, K., Wang, L., Handa, J.T. (2017). The impact of oxidative stress and inflammation on RPE degeneration in non-neovascular AMD. *Prog Retin Eye Res*, 60, 201-218.

- [2] Wong, W.L., Su, X., Li, X., Cheung, C.M.G., Klein, R., Cheng, C.-Y., Wong, T.Y. (2014). Global prevalence of age-related macular degeneration and disease burden projection for 2020 and 2040: a systematic review and meta-analysis. *Lancet Glob Health*, 2(2), e106-e116.
- [3] Lambert, N.G., ElShelmani, H., Singh, M.K., Mansergh, F.C., Wride, M.A., Padilla, M., Keegan, D., Hogg, R.E., Ambati, B.K. (2016). Risk factors and biomarkers of age-related macular degeneration. *Prog Retin Eye Res*, 54, 64-102.
- [4] van Lookeren Campagne, M., LeCouter, J., Yaspan, B.L., Ye, W. (2014). Mechanisms of age-related macular degeneration and therapeutic opportunities. *J Pathol*, 232(2), 151-164.
- [5] Bowes Rickman, C., Farsiu, S., Toth, C.A., Klingeborn, M. (2013). Dry age-related macular degeneration: mechanisms, therapeutic targets, and imaging. *Invest Ophthalmol Vis Sci*, 54(14), ORSF68-80.
- [6] Ding, X., Patel, M., Chan, C.C. (2009). Molecular pathology of age-related macular degeneration. *Prog. Retin. Eye Res*, 28(1), 1-18.
- [7] Zarbin, M.A. (2004). Current concepts in the pathogenesis of age-related macular degeneration. *Arch Ophthalmol*, 122(4), 598-614.
- [8] Ach, T., Tolstik, E., Messinger, J.D., Zarubina, A.V., Heintzmann, R., Curcio, C.A. (2015). Lipofuscin redistribution and loss accompanied by cytoskeletal stress in retinal pigment epithelium of eyes with age-related macular degeneration. *Invest Ophthalmol Vis Sci*, 56(5), 3242-3252.
- [9] Cai, J., Nelson, K.C., Wu, M., Sternberg, P.Jr., Jones, D.P. (2000). Oxidative damage and protection of the RPE. *Prog Retin Eye Res*, 19(2), 205-221.
- [10] Lambros, M.L., Plafker, S.M. (2016). Oxidative stress and the Nrf2 anti-oxidant transcription factor in age-related macular degeneration. *Adv Exp Med Biol*, 854, 67-72.

- [11] Mao, H., Seo, S.J., Biswal, M.R., Li, H., Conners, M., Nandyala, A., Jones, K., Le, Y.Z., Lewin, A.S. (2014). Mitochondrial oxidative stress in the retinal pigment epithelium leads to localized retinal degeneration. *Invest Ophthalmol Vis Sci*, 55(7), 4613-4627.
- [12] Sachdeva, M.M., Cano, M., Handa, J.T. (2014). Nrf2 signaling is impaired in the aging RPE given an oxidative insult. *Exp Eye Res*, 119, 111-114.
- [13] Comer, G.M., Ciulla, T.A., Heier, J.S., Criswell, M.H. (2005). Future pharmacological treatment options for nonexudative and exudative age-related macular degeneration. *Expert Opin Emerg Drugs*, 10(1), 119-135.
- [14] Michels, S., Garhöfer, G. (2016). Nonneovascular age-related macular degeneration. *Dev Ophthalmol*, 55, 112-124.
- [15] Dieguez, H.H., Romeo, H.E., González Fleitas, M.F., Aranda, M.L., Milne, G.A., Rosenstein, R.E., Dorfman, D. (2018). Superior cervical gangliectomy induces non-exudative age-related macular degeneration in mice. *Dis Model Mech*, 11(2), pii: dmm031641.
- [16] Dieguez, H.H., Romeo, H.E., Alaimo, A., González Fleitas, M.F., Aranda, M.L., Rosenstein, R.E., Dorfman, D. (2019). Oxidative stress damage circumscribed to the central temporal retinal pigment epithelium in early experimental non-exudative age-related macular degeneration. *Free Radic Biol Med*, 131, 72-80.
- [17] Escribano, B.M., Colín-González, A.L., Santamaría, A., Túnez, I. (2014). The role of melatonin in multiple sclerosis, Huntington's disease and cerebral ischemia. *CNS Neurol Disord Drug Targets*, 13(6), 1096-1119.
- [18] García, J.J., López-Pingarrón, L., Almeida-Souza, P., Tres, A., Escudero, P., García-Gil, F.A., Tan, D.X., Reiter, R.J., Ramírez, J.M., Bernal-Pérez, M. (2014). Protective effects of melatonin in reducing oxidative stress and in preserving the fluidity of biological membranes: a review. *J Pineal Res*, 56(3), 225-237.

- [19] Mauriz, J.L., Collado, P.S., Veneroso, C., Reiter, R.J., González-Gallego, J. (2013). A review of the molecular aspects of melatonin's anti-inflammatory actions: recent insights and new perspectives. *J Pineal Res*, 54(1), 1-14.
- [20] Galano, A., Tan, D.X., Reiter, R.J. (2013). On the free radical scavenging activities of melatonin's metabolites, AFMK and AMK. *J Pineal Res*, 54(3), 245-257.
- [21] Manchester, L.C., Coto-Montes, A., Boga, J.A., Andersen, L.P., Zhou, Z., Galano, A., Vriend, J., Tan, D.X., Reiter, R.J. (2015). Melatonin: an ancient molecule that makes oxygen metabolically tolerable. *J Pineal Res*, 59(4), 403-419.
- [22] Reiter, R.J., Paredes, S.D., Manchester, L.C., Tan, D.X. (2009). Reducing oxidative/nitrosative stress: a newly-discovered genre for melatonin. *Crit Rev Biochem Mol Biol*, 44(4), 175-200.
- [23] Rodriguez, C., Mayo, J.C., Sainz, R.M., Antolín, I., Herrera, F., Martín, V., Reiter, R.J. (2004). Regulation of antioxidant enzymes: a significant role for melatonin. *J Pineal Res*, 36(1), 1-9.
- [24] Zhang, H.M., Zhang, Y. (2014). Melatonin: a well-documented antioxidant with conditional pro-oxidant actions. *J Pineal Res*, 57(2), 131-146.
- [25] Ciuffi, M., Pisanello, M., Pagliai, G., Raimondi, L., Franchi-Micheli, S., Cantore, M., Mazzetti, L., Failli, P. (2003). Antioxidant protection in cultured corneal cells and whole corneas submitted to UV-B exposure. *J Photochem Photobiol B*, 71(1-3), 59-68.
- [26] Sande, P.H., Álvarez, J., Calcagno, J., Rosenstein, R.E. (2016). Preliminary findings on the effect of melatonin on the clinical outcome of cataract surgery in dogs. *Vet Ophthalmol*, 19(3), 184-194.
- [27] Siu, A.W., Maldonado, M., Sanchez-Hidalgo, M., Tan, D.X., Reiter, R.J. (2006). Protective effects of melatonin in experimental free radical-related ocular diseases. *J Pineal Res*, 40(2), 101-109.

- [28] Gramajo, A.L., Marquez, G.E., Torres, V.E., Juárez, C.P., Rosenstein, R.E., Luna, J.D. (2015). Therapeutic benefit of melatonin in refractory central serous chorioretinopathy. *Eye (Lond)*, 29(8), 1036-1045.
- [29] Belforte, N.A., Moreno, M.C., de Zavalía, N., Sande, P.H., Chianelli, M.S., Keller Sarmiento, M.I., Rosenstein, R.E. (2010). Melatonin: a novel neuroprotectant for the treatment of glaucoma. *J Pineal Res*, 48(4), 353-364.
- [30] Del Sole, M.J., Sande, P.H., Fernandez, D.C., Sarmiento, M.I., Aba, M.A., Rosenstein, R.E. (2012). Therapeutic benefit of melatonin in experimental feline uveitis. *J Pineal Res*, 52(1), 29-37.
- [31] Sande, P.H., Fernandez, D.C., Aldana Marcos, H.J., Chianelli, M.S., Aisemberg, J., Silberman, D.M., Sáenz, D.A., Rosenstein, R.E. (2008). Therapeutic effect of melatonin in experimental uveitis. *Am J Pathol*, 173(6), 1702-1713.
- [32] Sande, P.H., Dorfman, D., Fernandez, D.C., Chianelli, M., Domínguez Rubio, A.P., Franchi, A.M., Silberman, D.M., Rosenstein, R.E., Sáenz, D.A. (2014). Treatment with melatonin after onset of experimental uveitis attenuates ocular inflammation. *Br J Pharmacol*, 171(24), 5696-5707.
- [33] Salido, E.M., Bordone, M., De Laurentiis, A., Chianelli, M., Keller Sarmiento, M.I., Dorfman, D., Rosenstein, R.E. (2013). Therapeutic efficacy of melatonin in reducing retinal damage in an experimental model of early type 2 diabetes in rats. *J Pineal Res*, 54(2), 179-189.
- [34] Aranda, M.L., González Fleitas, M.F., De Laurentiis, A., Keller Sarmiento, M.I., Chianelli, M., Sande, P.H., Dorfman, D., Rosenstein RE. (2016). Neuroprotective effect of melatonin in experimental optic neuritis in rats. *J Pineal Res*, 60(3), 360-372.
- [35] Lim, J.H., Stafford, B.K., Nguyen, P.L., Lien, B.V., Wang, C., Zukor, K., He, Z., Huberman, A.D. (2016). Neural activity promotes long-distance, target-specific regeneration of adult retinal axons. *Nat Neurosci*, 19(8), 1073-1084.

- [36] Gu, L., Bok, D., Yu, F., Caprioli, J., Piri, N. (2018). Downregulation of splicing regulator RBFOX1 compromises visual depth perception. *PLoS One*, 13(7), e0200417.
- [37] Lowry, O.H., Rosebrough, N.J., Farr, A.L., Randall, R.J. (1951). Protein measurement with the Folin phenol reagent. *J Biol Chem*, 193(1), 265-275.
- [38] Steinle, J.J., Pierce J.D., Clancy R.L., Smith G.P. (2002). Increased ocular blood vessel numbers and sizes following chronic sympathectomy in rat. *Exp Eye Res* 74, 761-768.
- [39] Volland S, Esteve-Rudd J, Hoo J, Yee C, Williams DS (2015) A comparison of some organizational characteristics of the mouse central retina and the human macula. *PLoS One* 10: e0125631. doi: 10.1371/journal.pone.0125631.
- [40] Yilmaz, M., Meister, M. (2013). Rapid innate defensive responses of mice to looming visual stimuli. *Curr Biol*, 23(20), 2011-2015.
- [41] Fox, M.W. (1965). The visual cliff test for the study of visual depth perception in the mouse. *Anim Behav*, 13(2), 232-233.
- [42] Booij, J.C., Baas, D.C., Beisekeeva, J., Gorgels, T.G., Bergen, A.A. (2010). The dynamic nature of Bruch's membrane. *Prog Retin Eye Res*, 29(1), 1-18.
- [43] Bhutto, I., Lutty, G. (2012). Understanding age-related macular degeneration (AMD): relationships between the photoreceptor/retinal pigment epithelium/Bruch's membrane/choriocapillaris complex. *Mol Aspects Med*, 33(4), 295-317.
- [44] Karampelas, M., Sim, D.A., Keane, P.A., Papastefanou, V.P., Sadda, S.R., Tufail, A., Dowler, J. (2013). Evaluation of retinal pigment epithelium-Bruch's membrane complex thickness in dry age-related macular degeneration using optical coherence tomography. *Br J Ophthalmol*, 97(10), 1256-1261.
- [45] Dayhaw-Barker, P. (2002). Retinal pigment epithelium melanin and ocular toxicity. *Int J Toxicol*, 21(6), 451-454.

- [46] Feher, J., Kovacs, I., Artico, M., Cavallotti, C., Papale, A., Balacco Gabrieli, C. (2006). Mitochondrial alterations of retinal pigment epithelium in age-related macular degeneration. *Neurobiol Aging*, 27(7), 983-993.
- [47] Karunadharm, P.P., Nordgaard, C.L., Olsen, T.W., Ferrington, D.A. (2010). Mitochondrial DNA damage as a potential mechanism for age-related macular degeneration. *Invest Ophthalmol Vis Sci*, 51(11), 5470-5479.
- [48] Blasiak, J., Synowiec, E., Salminen, A., Kaarniranta, K. (2012). Genetic variability in DNA repair proteins in age-related macular degeneration. *Int J Mol Sci*, 13(10), 13378-13397.
- [49] Blasiak, J., Glowacki, S., Kauppinen, A., Kaarniranta, K. (2013). Mitochondrial and nuclear DNA damage and repair in age-related macular degeneration. *Int J Mol Sci*, 14(2), 2996-3010.
- [50] Fu, Y., Tang, M., Fan, Y., Zou, H., Sun, X., Xu, X. (2012). Anti-apoptotic effects of melatonin in retinal pigment epithelial cells. *Front Biosci (Landmark Ed)*, 17:1461-1468.
- [51] Liang, F.Q., Green, L., Wang, C., Alssadi, R., Godley, B.F. (2004). Melatonin protects human retinal pigment epithelial (RPE) cells against oxidative stress. *Exp Eye Res*, 78(6), 1069-1075.
- [52] Osborne, N.N., Nash, M.S., Wood, J.P. (1998). Melatonin counteracts ischemia-induced apoptosis in human retinal pigment epithelial cells. *Invest Ophthalmol Vis Sci*, 39(12), 2374-2383.
- [53] Rosen, R.B., Hu, D.N., Chen, M., McCormick, S.A., Walsh, J., Roberts, J.E. (2012). Effects of melatonin and its receptor antagonist on retinal pigment epithelial cells against hydrogen peroxide damage. *Mol Vis*, 18, 1640-1648.
- [54] Yu, L., Gong, B., Duan, W., Fan, C., Zhang, J., Li, Z., Xue, X., Xu, Y., Meng, D., Li, B., Zhang, M., Bin Zhang., Jin, Z., Yu, S., Yang, Y., Wang, H. (2017). Melatonin ameliorates myocardial ischemia/reperfusion injury in type 1 diabetic rats by preserving mitochondrial function: role of AMPK-PGC-1 α -SIRT3 signaling. *Sci Rep*, 7, 41337.

[55] Chang, C.C., Huang, T.Y., Chen, H.Y., Huang, T.C., Lin, L.C., Chang, Y.J., Hsia, S.M. (2018). Protective effect of melatonin against oxidative stress-induced apoptosis and enhanced autophagy in human retinal pigment epithelium cells. *Oxid Med Cell Longev*, 2018, 9015765.

[56] Yan, G., Yu, L., Jiang, S., Zhu, J. (2018). Melatonin antagonizes oxidative stress-induced mitochondrial dysfunction in retinal pigmented epithelium cells via melatonin receptor 1 (MT1). *J Toxicol Sci*, 43(11), 659-669.

[57] Reiter, R.J., Tan, D.X., Manchester, L.C., Pilar Terron, M., Flores, L.J., Koppisepi, S. (2007). Medical implications of melatonin: receptor-mediated and receptor-independent actions. *Adv Med Sci*, 52, 11-28.

[58] Reiter, R.J., Tan, D.X., Fuentes-Broto, L. (2010). Melatonin: a multitasking molecule. *Prog Brain Res*, 181, 127-151.

[59] Yi, C., Pan, X., Yan, H., Guo, M., Pierpaoli, W. (2005). Effects of melatonin in age-related macular degeneration. *Ann N Y Acad Sci*, 1057, 384-392.

[60] Andersen, L.P., Werner, M.U., Rosenkilde, M.M., Fenger, A.Q., Petersen, M.C., Rosenberg, J., Gögenur, I. (2016). Pharmacokinetics of high-dose intravenous melatonin in humans. *J Clin Pharmacol*, 56(3), 324-329.

FIGURE LEGENDS

Figure 1. Effect of melatonin on visual function alterations at 10 weeks post-SCGx. Panel A: The average amplitudes of scotopic ERG a-wave are shown. SCGx induced a significant decrease in ERG a-wave amplitude, whereas a treatment with melatonin starting 48 h post-SCGx, which had no effect *per se*, completely prevented the decrease in this parameter. Data are mean \pm S.E.M. (n: 10 animals per group), $**P < 0.01$ vs. sham-treated eyes from control (without melatonin) animals; a: $P < 0.01$, and b: $P < 0.05$ vs. SCGx-treated eyes from control animals, by Tukey's test. Panel B: Representative scotopic ERG traces of sham- and SCGx-eyes in control- and melatonin-treated animals. Panel C: The average responses in three behaviour visual tasks are shown. SCGx induced a significant increase in the freezing latency of the looming test, and a significant decrease both in the percentage of time spent on the shallow side in the virtual visual cliff test and the fraction of shallow-side selected trials in the visual cliff test, which were prevented by melatonin treatment. Data are mean \pm S.E.M. (n: 10 animals per group), $**P < 0.01$ vs. control animals with sham-treated eyes; a: $P < 0.01$, and b: $P < 0.05$ vs. control animals with SCGx-treated eyes, by Tukey's test.

Figure 2. Effect of melatonin on the choriocapillaris thickening induced by SCGx at 10 weeks post-surgery. SCGx induced a ubiquitous (i.e. the central nasal and temporal region) significant increase in the choriocapillaris lumen height increase (light-blue colouring) both in control and melatonin-treated animals. Shown are representative photomicrographs from 5 animals/group. Ch, choriocapillaris; Scale bar = 1 μ m. Data are mean \pm S.E.M. (n: 5 animals per group), $**P < 0.01$ vs. sham-treated eyes from control animals, by Tukey's test.

Figure 3. Effect of melatonin on the Bruch's membrane damage found at 10 weeks post-SCGx. Transverse ultrathin sections from control eyes and SCGx-eyes at 10 weeks post-surgery. SCGx induced a temporal (but not nasal) BrM thickening, a clear loss of its pentalaminar structure (asterisk), and thickening of the endothelial cell basal membrane (arrowhead), whereas BrM structure and thickness in SCGx-treated eyes from animals treated with melatonin were similar to sham-treated eyes from control animals. Shown are representative photomicrographs at 800 μ m, nasally and temporally from the ONH, from 5 eyes/group. BM, basal membrane; IC, internal collagenous layer; EL, elastic layer; OC, outer collagenous layer; Ch, choriocapillaris. Scale bar = 200 nm. Data are mean \pm S.E.M. (n: 5 eyes per group), $**P < 0.01$ vs. sham-treated eyes from control animals; a: $P < 0.01$ vs. SCGx-eyes from control animals, by Tukey's test.

Figure 4. Effect of melatonin on the decrease in the RPE melanin content and melanosome number induced by SCGx. Panel A: Representative photomicrographs showing a decrease in RPE melanin content (arrow) and melanosome number at the central temporal (but not nasal) RPE in SCGx-treated eyes from control animals. The treatment with melatonin completely prevented these alterations (quantified in panel B). OS, photoreceptor outer segments; RPE, retinal pigment epithelium; Ch, choroid. Scale bars = 25 μ m and 1 μ m. Data are mean \pm S.E.M. (n: 5 eyes per group), $**P < 0.01$ vs. sham-treated eyes from animals control (without melatonin); b: $P < 0.05$ vs. SCGx-treated eyes from control animals, by Tukey's test.

Figure 5. Effect of melatonin on the decrease in RPE65-immunoreactivity induced by SCGx. Representative RPE photomicrographs of RPE65 immunostaining at the central nasal and temporal RPE. Melatonin significantly prevented the decrease in RPE65 immunostaining at the temporal (but not nasal) RPE at 10 weeks post-SCGx (arrowhead). Shown are representative photomicrographs from 5 eyes/group. OS, photoreceptor outer segments; RPE, retinal pigment epithelium; Ch, choroid. Scale bar = 25 μ m. Data are mean \pm S.E.M. (n: 5 eyes per group), $**P < 0.01$ vs. sham-treated eyes from control animals (without melatonin); a: $P < 0.01$ vs. SCGx-treated eyes from control animals, by Tukey's test.

Figure 6. Effect of melatonin on the RPE and PR ultrastructure alterations induced by SCGx. Representative transverse ultrathin RPE and PR sections from sham treated eyes, and eyes at 10 weeks post-SCGx from control and melatonin-treated animals. Superior panel: Melatonin prevented the vacuolization of the temporal RPE (arrow), the thickening of the RPE basal infoldings (arrowhead). Shown are representative photomicrographs from 5 eyes/group. OS, photoreceptors outer segments; RPE, retinal pigment epithelium; BI, basal infoldings. Scale bar = 500 nm. Lower panel: SCGx induced focal losses of the temporal (but not nasal) PR discs and blebs (asterisk), which were not observed in eyes from animals treated with melatonin. Shown are representative photomicrographs from 5 eyes/group. Scale bar = 100 nm. Data are mean \pm S.E.M. (n: 5 eyes per group), $**P < 0.01$ vs. sham-treated eyes from control animals (without melatonin); a: $P < 0.01$ vs. SCGx-treated eyes from control animals, by Tukey's test.

Figure 7. Effect of melatonin on the outer retina/RPE region-dependent oxidative damage at 6 weeks post-SCGx. 4HNE- and CML-immunostaining at the nasal and temporal outer retina and RPE. Melatonin prevented the SGCx-induced increase in 4HNE- and CML-immunoreactivity at the temporal outer retina/RPE (arrow), and RPE (arrowhead) respectively. Shown are photomicrographs representative from 5

eyes/group. ONL, outer nuclear layer; IS, photoreceptor inner segments; OS, photoreceptor outer segments; RPE, retinal pigment epithelium; Chr, choroid. Scale bar: 50 μ m.

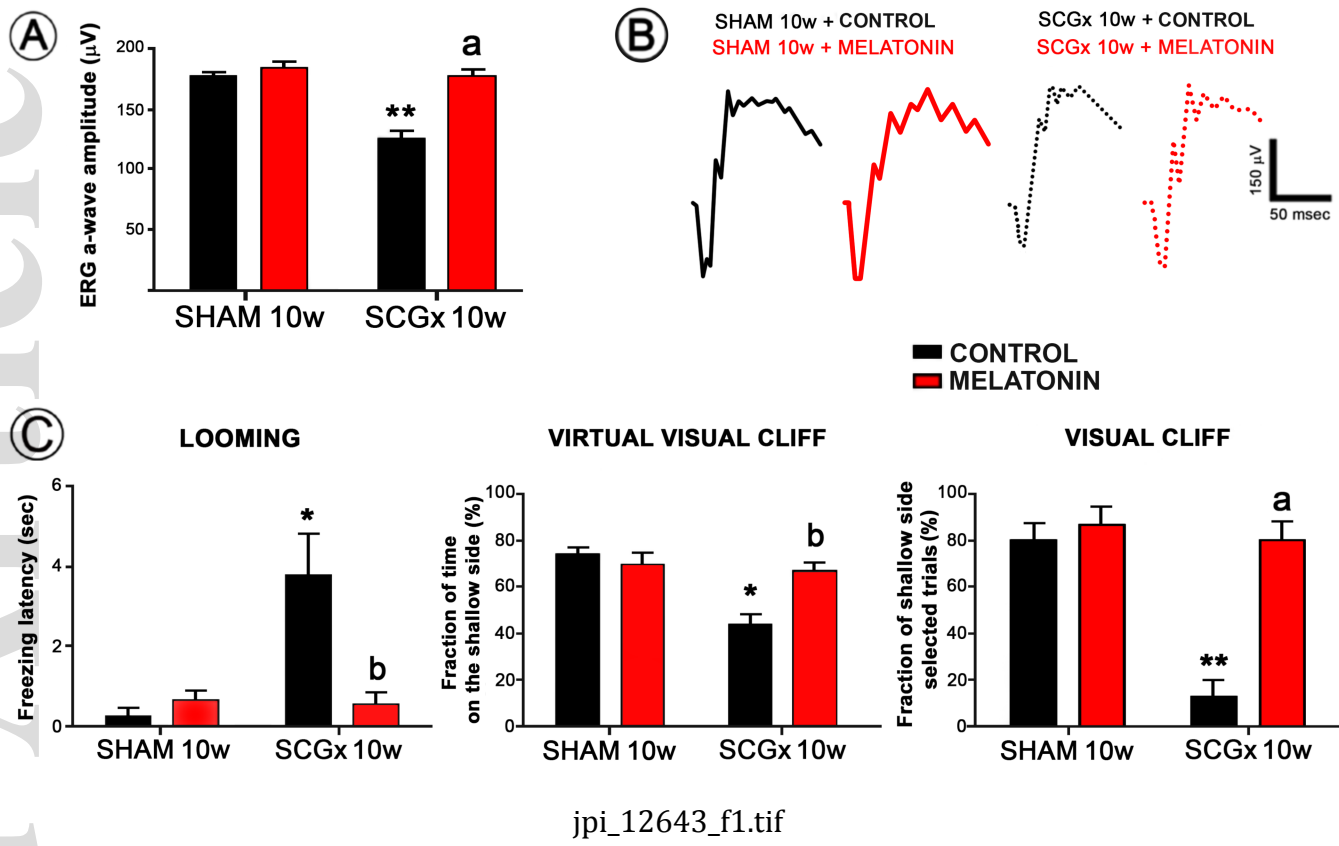
Figure 8. Effect of melatonin on the increase of mitochondria superoxide and the decrease in the mass of the temporal RPE mitochondria induced at 6 weeks post-SCGx. Panel A: MitoSox-Red-labeled mitochondria in the central nasal and temporal RPE flat-mounts. The treatment with melatonin significantly prevented (quantified in panel C) the SCGx-induced increase in MitoSox-Red-labeled mitochondria at the temporal RPE. Panel B: Mitotracker-Red-labeled mitochondria in the central nasal and temporal RPE flat-mounts. SCGx induced a significant decrease (quantified in panel C) in Mitotracker-Red(+) puncta at the temporal RPE, which was prevented in SCGx-treated eyes from animals with melatonin. No differences regarding Mitotracker-Red(+) and MitoSox-Red puncta were observed between experimental groups at the nasal side (data not shown). Shown are photomicrographs representative from 4 eyes/group. Scale bars = 25 μ m. Data are mean \pm S.E.M. (n: 4 eyes per group), $**P < 0.01$ vs. sham-treated eyes from control animals; a: $P < 0.01$ vs. SCGx-treated eyes from control animals, by Tukey's test.

Figure 9. Effect of melatonin on the decreased levels of intrinsic mitochondria proteins at 6 weeks post-SCGx. Left panel: Representative Western blots for the assessment of mitochondria intrinsic proteins. SCGx, which had no effect on the nasal RPE, induced a decrease in the levels of cytochrome c, VDAC, and TOM20 at the temporal RPE. Melatonin, which did not have effects *per se*, prevented these alterations. The densitometric analysis is shown on the right. Data are mean \pm S.E.M. (n: 4 homogenates per group), $**P < 0.01$, $*P < 0.05$ vs. sham-treated eyes from control animals; a: $P < 0.01$, b: $P < 0.05$ vs. SCGx-treated eyes from control animals, by Tukey's test.

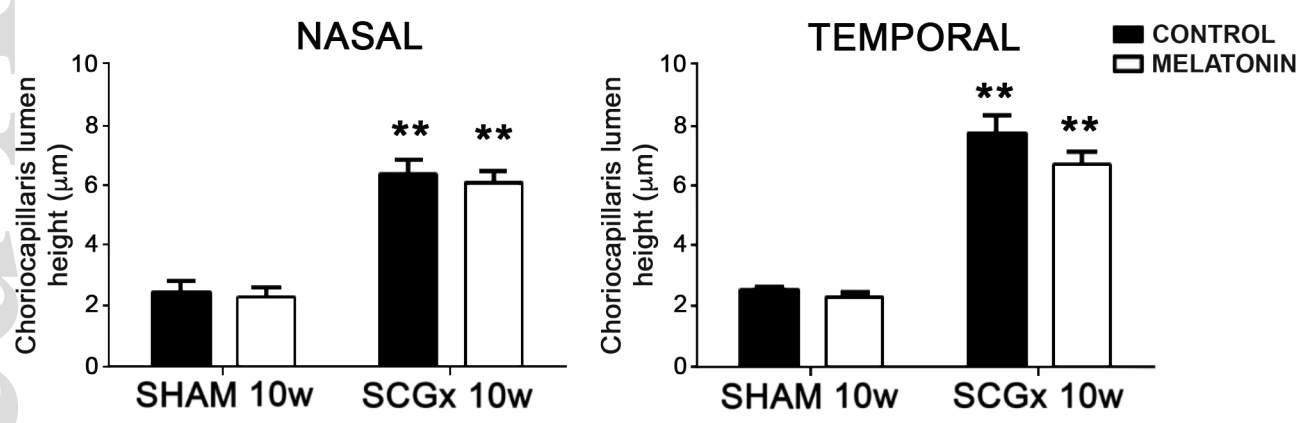
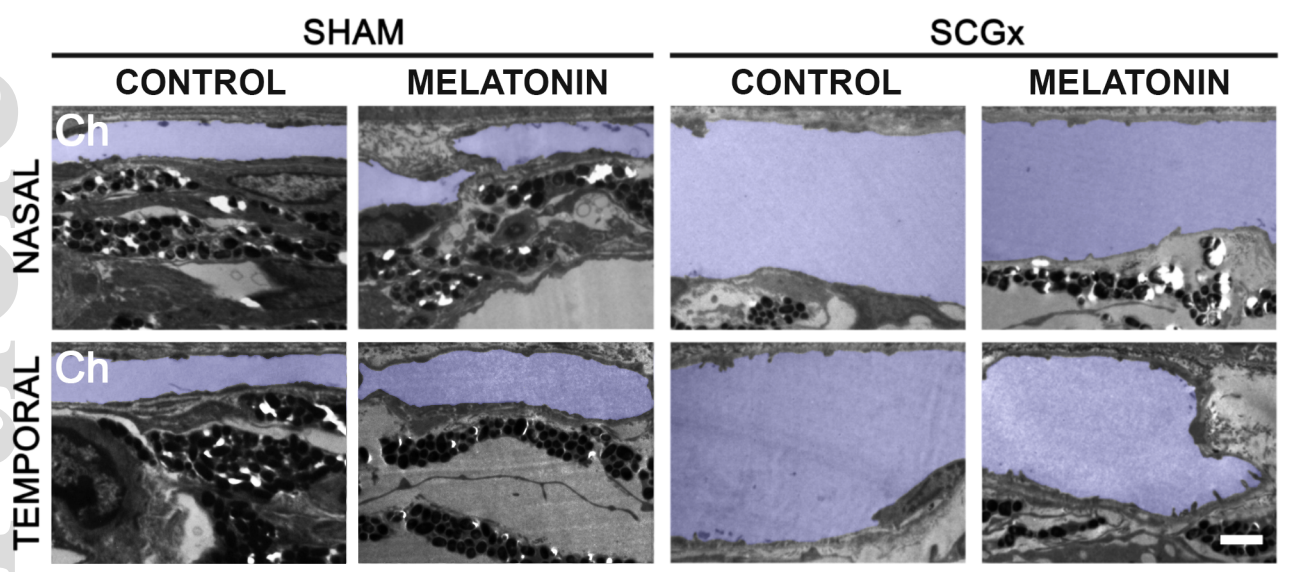
Figure 10. Effect of the delayed treatment with melatonin on the visual function alterations induced by SCGx. Panel A: The average amplitudes of scotopic ERG a-wave is shown. Melatonin treatment starting at 4 weeks post-SCGx completely reversed the decrease in the ERG a-wave amplitude. Data are mean \pm S.E.M. (n: 10 animals per group), $**P < 0.01$ vs. sham-treated eyes from control animals; a: $P < 0.01$ vs. SCGx-treated eyes from control animals, by Tukey's test. Panel B: Representative scotopic ERG traces of sham- and SCGx- eyes from control and melatonin-treated animals. Panel C: The average responses in three behaviour visual tasks are shown. The delayed treatment with melatonin reversed the visual behaviour responses at 10 weeks post-SCGx. Data are mean \pm S.E.M. (n: 10 animals per group), $**P$

< 0.01, and b: $P < 0.05$ vs. control animals with sham-treated eyes; a: $P < 0.01$, and b: $P < 0.05$ vs. control animals with SCGx-treated eyes, by Tukey's test.

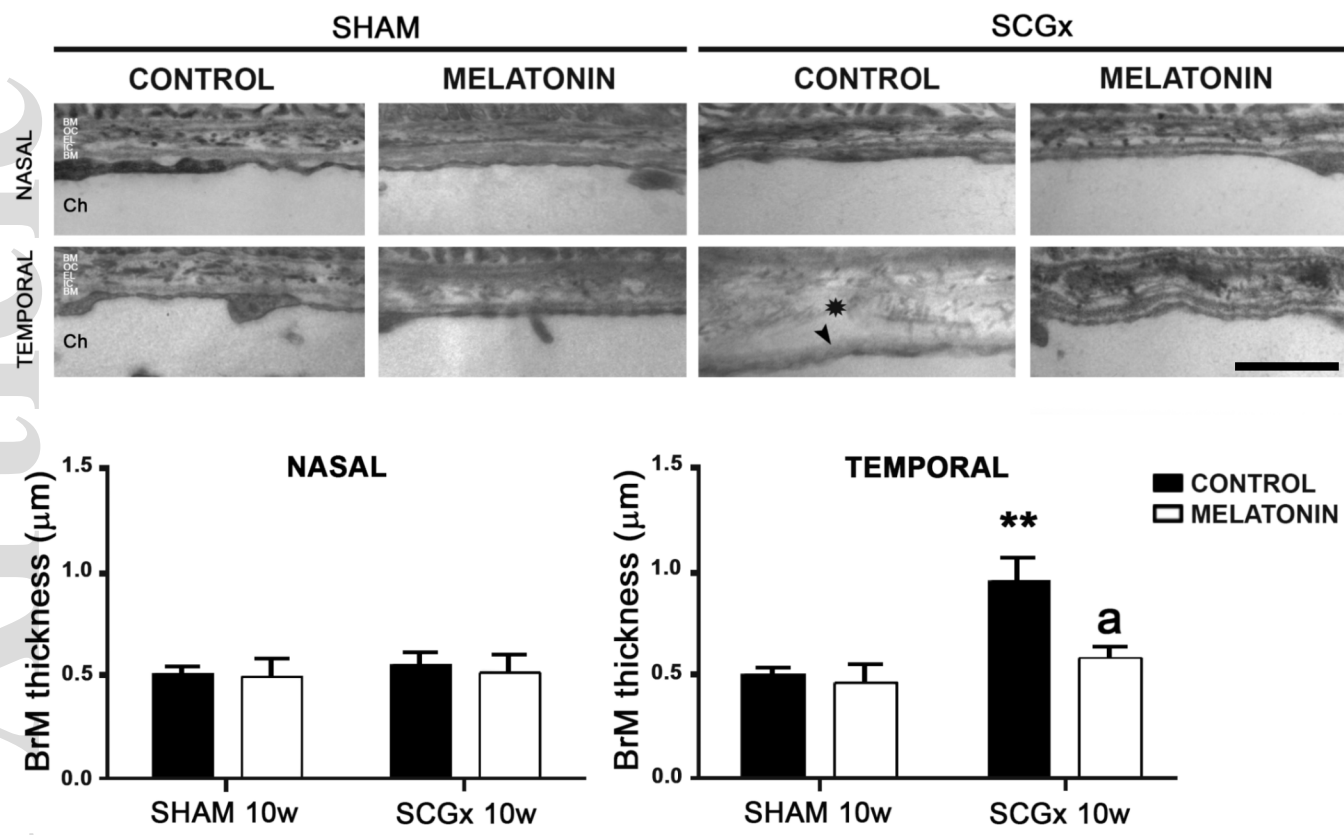
Figure 11. Effect of melatonin delayed-treatment on the decrease in the RPE melanin content and RPE65-immunoreactivity induced by SCGx. Panel A: Representative photomicrographs showing a significant decrease in RPE melanin content at the central temporal (but not nasal) RPE in SCGx-treated eyes from control animals (arrow), which was not observed in SCGx-eyes from animals treated with melatonin starting at 4 weeks post-SCGx. OS, photoreceptor outer segments; RPE, retinal pigment epithelium; Ch, choroid. Scale bar = 25 μm . Data are mean \pm S.E.M. (n: 5 eyes per group), $**P < 0.01$ vs. sham-treated eyes from animals without melatonin (control); b: $P < 0.05$ vs. SCGx-treated eyes from control animals, by Tukey's test. Panel B: Representative RPE photomicrographs of RPE65 immunostaining at the central nasal and temporal RPE. The delayed treatment with melatonin prevented the decrease in RPE65-immunoreactivity at 10 weeks post-SCGx (arrowhead). Shown are representative photomicrographs from 5 eyes/group. OS, photoreceptor outer segments; RPE, retinal pigment epithelium; Ch, choroid. Scale bar = 50 μm . Data are mean \pm S.E.M. (n: 5 eyes per group), $**P < 0.01$ vs. sham-treated eyes from animals without melatonin (control); a: $P < 0.01$ vs. SCGx-treated eyes from control animals, by Tukey's test.



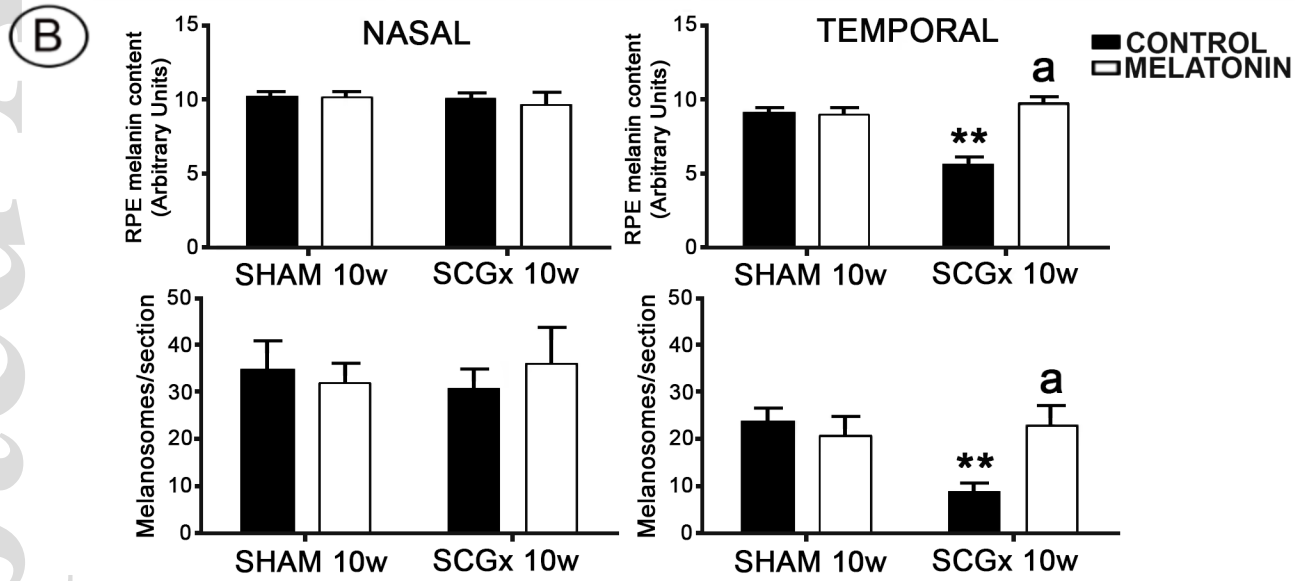
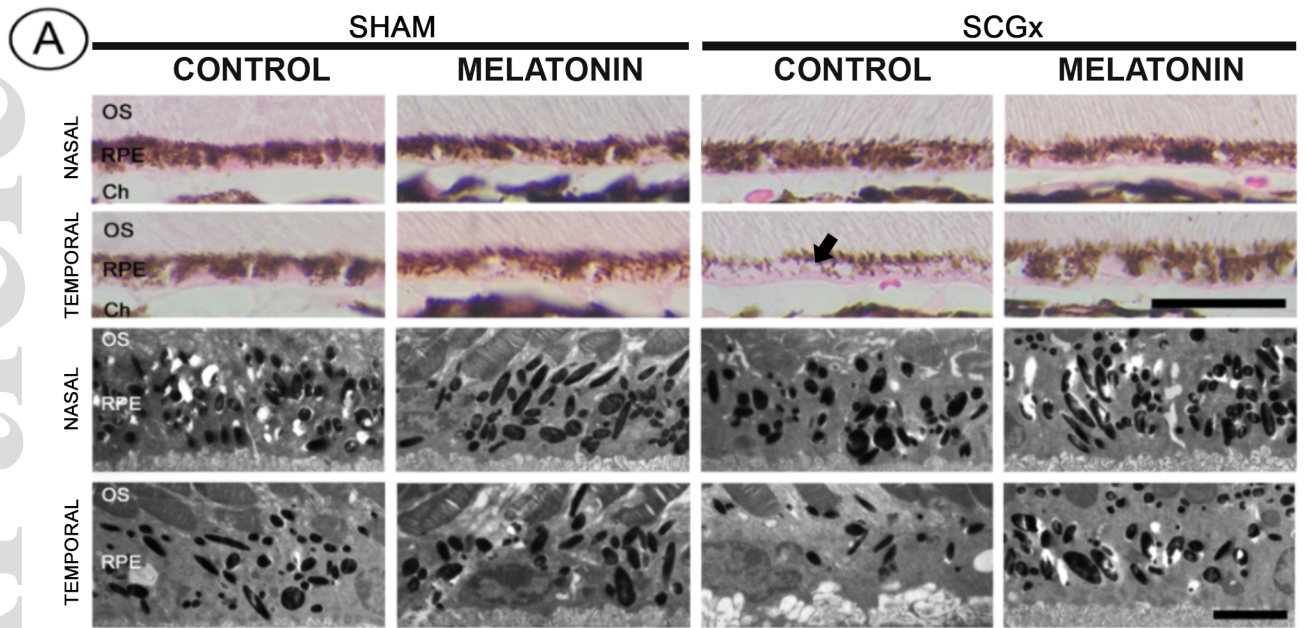
jpi_12643_f1.tif



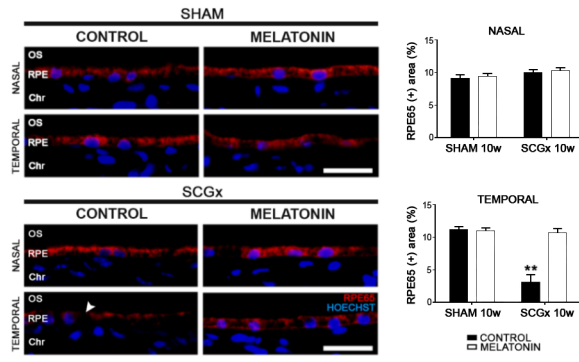
jpi_12643_f2.tif



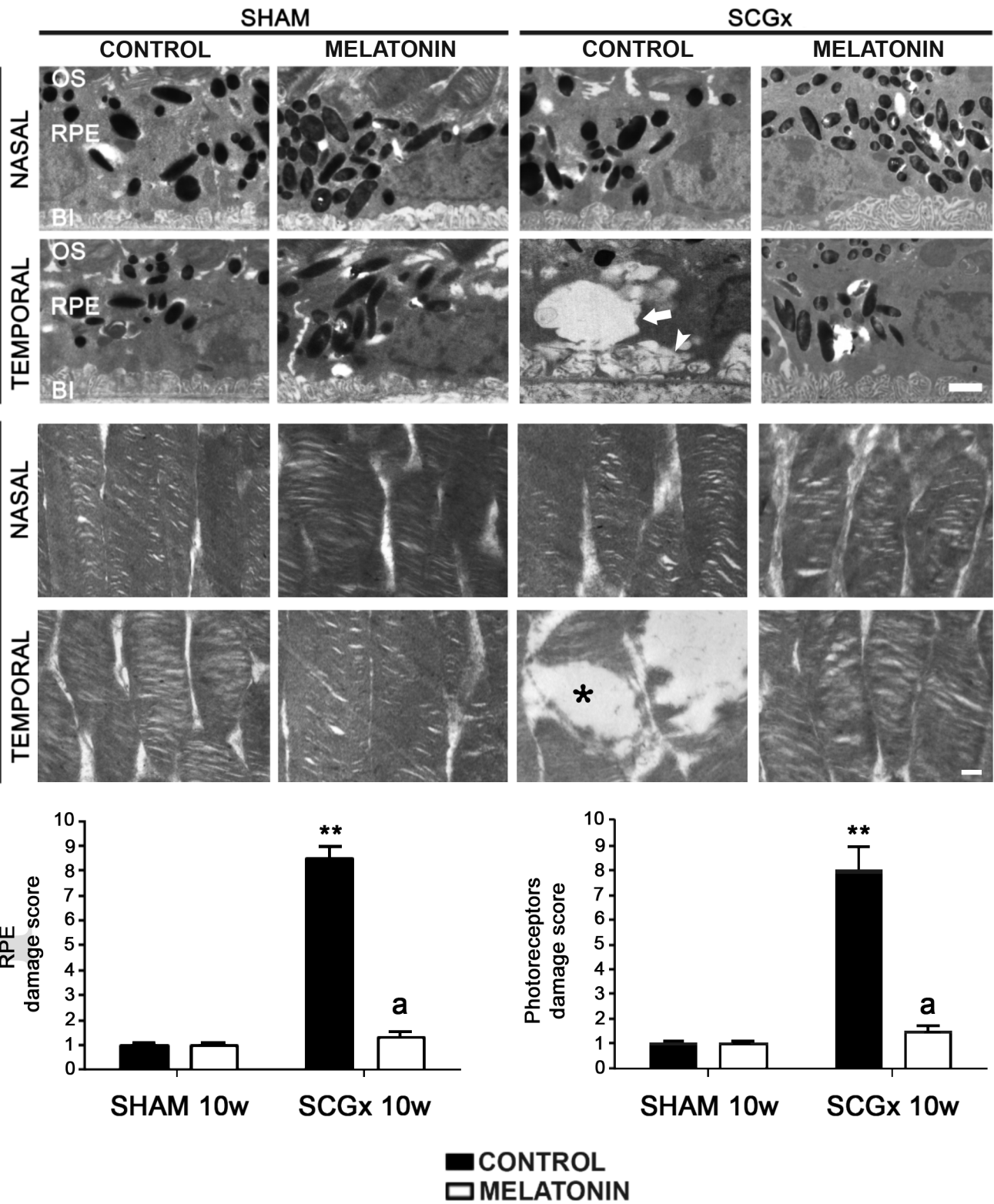
jpi_12643_f3.tif



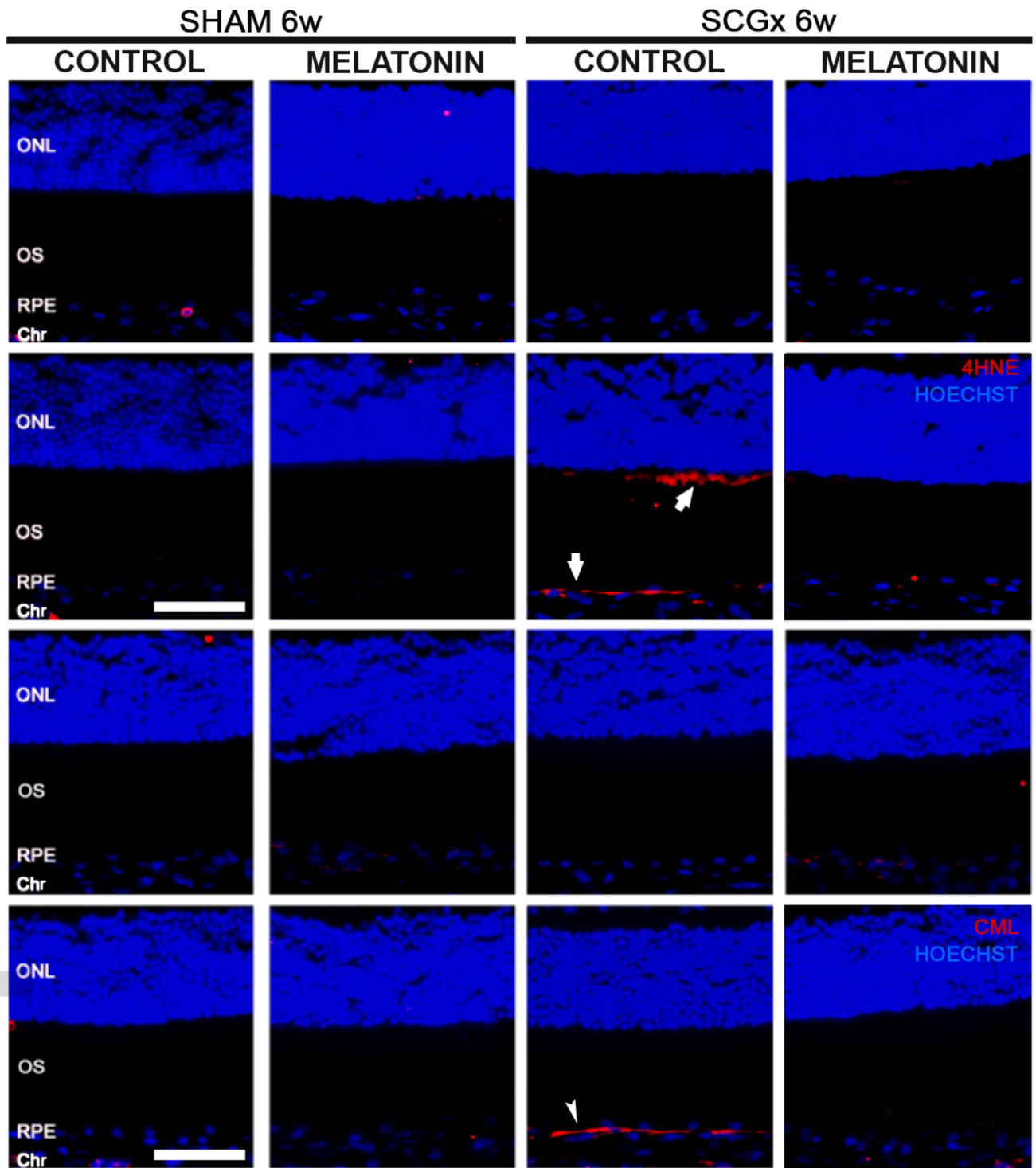
jpi_12643_f4.tif



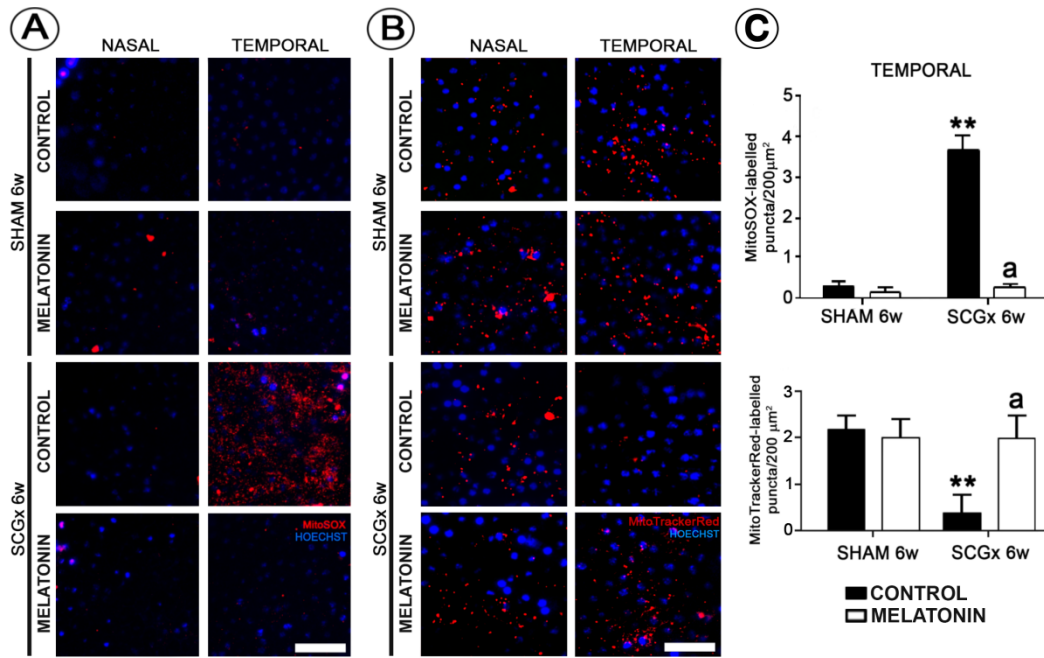
jpi_12643_f5.tif



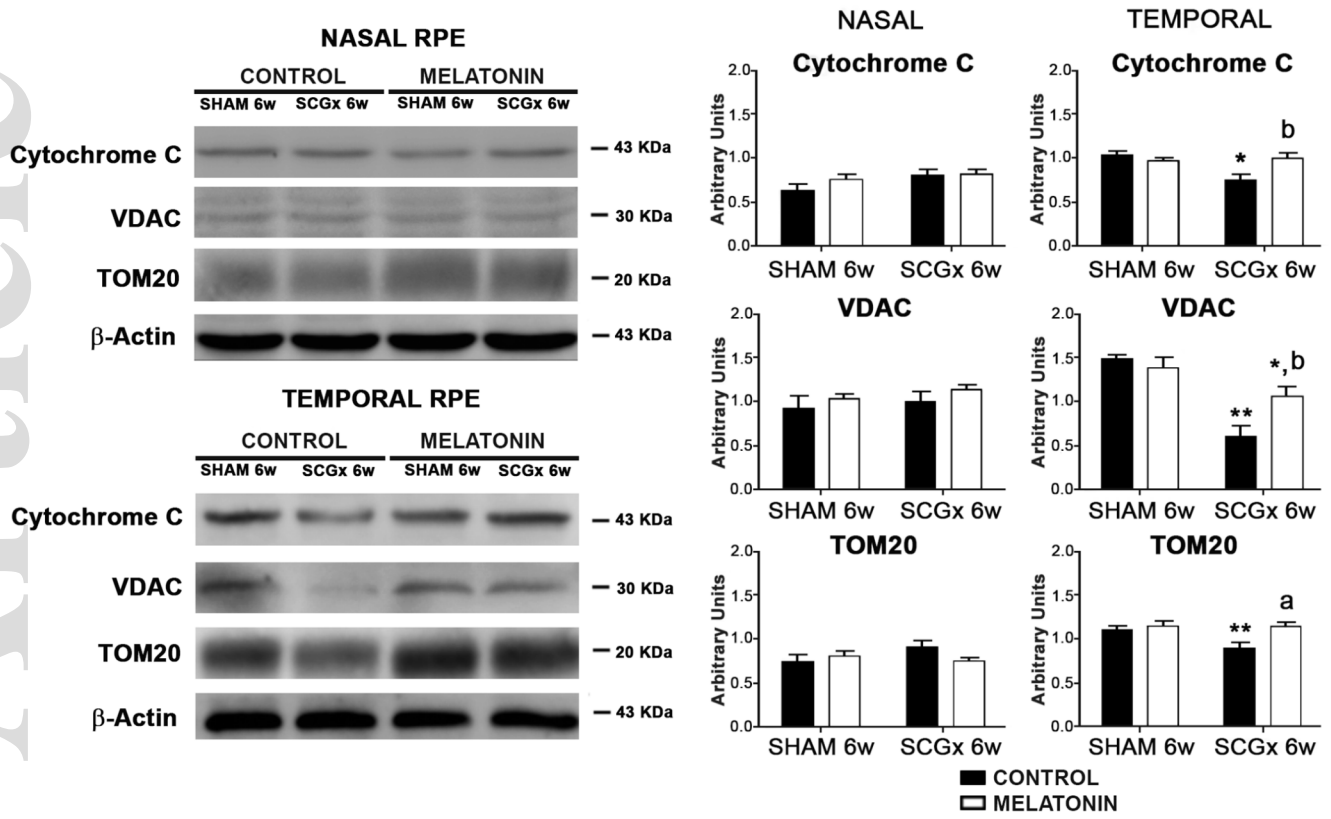
jpi_12643_f6.tif



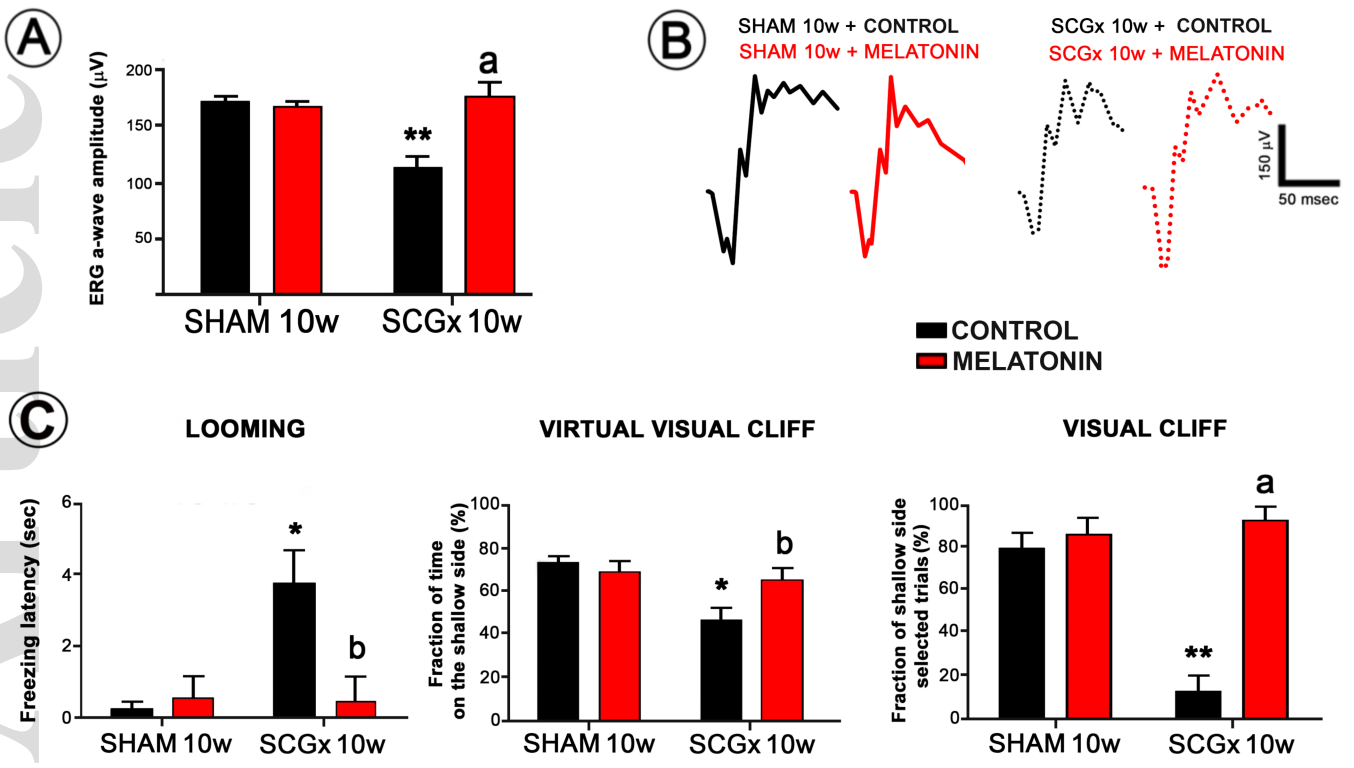
jpi_12643_f7.tif



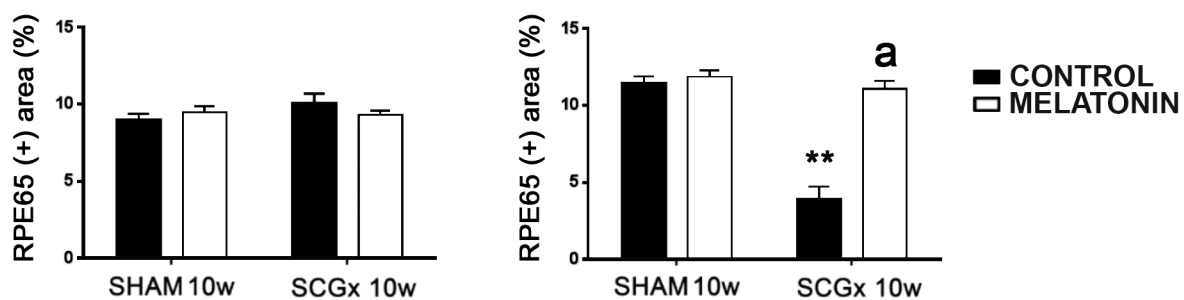
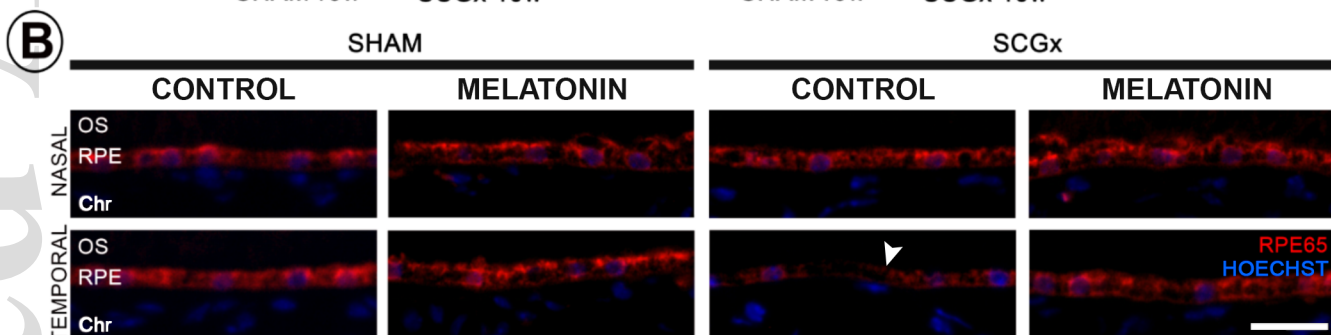
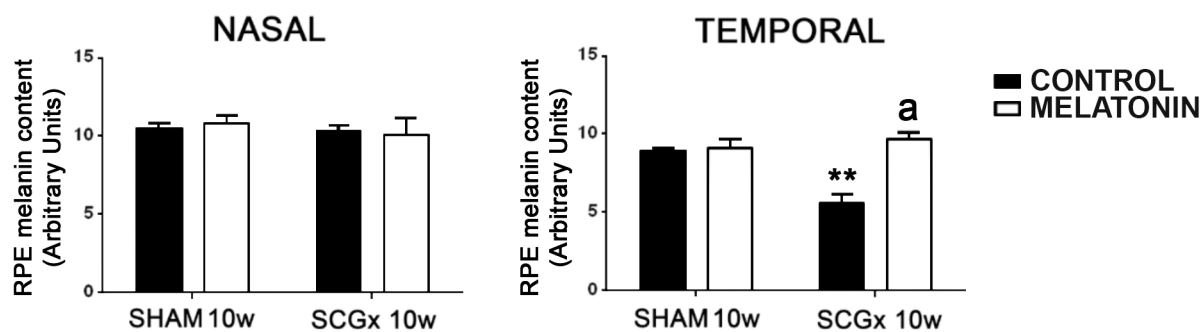
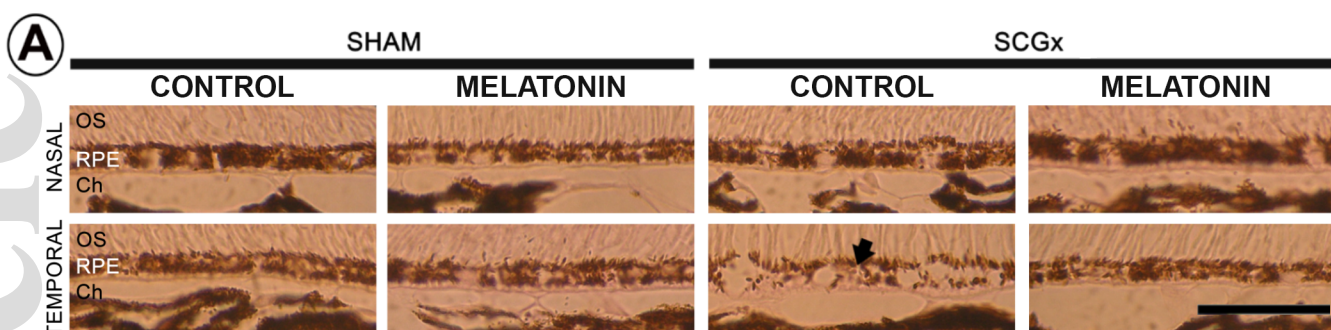
jpi_12643_f8.tif



jpi_12643_f9.tif



jpi_12643_f10.tif



jpi_12643_f11.tif